Identification of Novel p53 Target Genes in Ionizing Radiation Response

Kuang-Yu Jen and Vivian G. Cheung

Departments of Pediatrics and Genetics, University of Pennsylvania, The Children's Hospital of Philadelphia, Philadelphia, Pennsylvania

Abstract

The tumor suppressor p53 plays an essential role in cellular adaptation to stress. In response to ionizing radiation, p53 regulates the transcription of genes in a diverse set of pathways including DNA repair, cell cycle arrest, and apoptosis. Previously, we identified by microarray analysis a set of genes that are transcriptionally activated or repressed in response to radiation exposure. In this study, we use computational methods and molecular techniques, including location analysis (ChIP-on-chip assay), to identify ionizing radiation–responsive genes that are directly regulated by p53. Among the 489 ionizing radiation–responsive genes examined, 38 genes were found to be p53 targets. Some of these genes are previously known to be directly regulated by p53 whereas others are novel p53 targets. We further showed that the novel p53 target genes are transcriptionally regulated by p53. The binding of p53 to promoters of target genes correlated with increased transcript levels of these genes in cells with functional p53. However, p53 binding and subsequent transcriptional activation of these target genes were significantly diminished in cells with mutant p53 and in cells from patients with ataxia telangiectasia, which have impaired p53 activation following ionizing radiation exposure. Identification and characterization of ionizing radiation–responsive p53 target genes extend our knowledge of the diverse role that p53 plays in the DNA damage response. (Cancer Res 2005; 65(17): 7666-73)

Introduction

Humans are exposed to a variety of DNA damaging agents. In response to these genotoxic stresses, mammalian cells elicit an integrated network of events that function at both the protein and RNA levels to maintain genomic stability and ensure fidelity of genetic information. When DNA damage is not properly repaired, mutations accumulate, which can eventually lead to tumorigenesis.

Injury to DNA can result from exposure to a wide variety of agents including ionizing radiation, ultraviolet radiation, genotoxic chemicals, and oxidative sources. Specifically, ionizing radiation causes many types of DNA damage of which double-strand breaks are the most deleterious. Double-strand breaks not only contribute to the formation of chromosomal aberrations but can also compromise cell viability.

The first step in the cellular ionizing radiation response involves recognition of double-strand breaks. This signal activates DNA repair and halts cell cycle progression. Apoptosis is induced if the damage is too extensive for cell survival. The tumor suppressor p53 functions as a crucial transcription factor in response to many types of stresses. Following ionizing radiation exposure, p53 integrates and relays DNA damage signals to activate ionizing radiation–responsive pathways. The transcriptional regulatory activity of p53 is mediated through direct protein binding to its target genes. p53 regulates the expression of various genes involved in DNA repair, cell cycle progression, and cell death and coordinates these pathways to determine cell fate. Some well-characterized targets of p53 include *CDKN1A* (*p21*; ref. 1), *DDB2* (2), *GADD45A* (3), and the death receptors *TNFRSF6* (*Fas/Apo-1*; ref. 4) and *TNFRSF10B* (*DR5/KILLER;* ref. 5). Mutations which disrupt p53 function are one of the most common genetic alterations observed in human cancers (6).

Given that p53 plays a pivotal role in DNA damage response and tumor suppression, we explored the function of p53 as a transcription factor following ionizing radiation–induced DNA damage. Previously, we and others have identified a set of genes that are induced and/or repressed in response to ionizing radiation (7–9). Because p53 is essential in eliciting stress-induced transcriptional response, it is likely that some of the ionizing radiation–responsive genes are direct transcriptional targets of p53.

In this study, we identified ionizing radiation–responsive p53 target genes by location analysis (ChIP-on-chip assay). A subset of these genes were validated by traditional chromatin immunoprecipitation (ChIP) and luciferase reporter assays. We also show that cells expressing mutant p53 and ataxia telangiectasia mutated (ATM)–deficient cells that are inefficient in activating p53 were unable to regulate the expression levels of these ionizing radiation–responsive p53 target genes following radiation exposure.

Materials and Methods

Cell culture and treatment. Human lymphoblastoid cell lines (Coriell, Camden, NJ) from the Centre d'Etude du Polymorphisme Humain collection were grown at a density of 5×10^5 cells/mL in RPMI 1640 supplemented with 15% fetal bovine serum, 2 mmol/L L-glutamine, and 100 units/mL penicillin-streptomycin. Cells were γ-irradiated with ^{137}Cs irradiator at a dose of 10 Gy (and other doses as indicated in Supplementary Fig. 2) and harvested at various time points postirradiation. The human lung adenocarcinoma cell line H1299, expressing temperature-sensitive p53-Val138, was kindly provided by Dr. Donna George at the University of Pennsylvania. Cells were maintained at 37°C in DMEM supplemented with 10% fetal bovine serum, 2 mmol/L L-glutamine, 100 units/mL penicillin-streptomycin, and 0.75 mg/mL G418.

Chromatin immunoprecipitation. ChIP was done in a similar manner as previously described (10–12). Briefly, cells were fixed with 0.5% formaldehyde for 10 minutes at room temperature and neutralized with 125 mmol/L glycine for 5 minutes. Cells were washed twice with PBS and resuspended in lysis buffer [10 mmol/L Tris-Cl (pH 8.0), 10 mmol/L

Note: Supplementary data for this article are available at Cancer Research Online (http://cancerres.aacrjournals.org/).

Requests for reprints: Vivian G. Cheung, Department of Pediatrics, University of Pennsylvania, 3615 Civic Center Boulevard, ARC 516G, Philadelphia, PA 19104. Phone: 215-590-4950; E-mail: vcheung@mail.med.upenn.edu.

doi:10.1158/0008-5472.CAN-05-1039

Table 1. Genomic regions physically associated with p53

Accession no.	Gene	Probe position	4 h		24 h	
			Mean ratio	*P*	Mean ratio	*P*
Apoptosis						
NM_138765	*BAX*	+438 to +1,574	4.3	1.5e−11	ns	ns
NM_014417	*BBC3*	−1,777 to −1,262	6.8	8.4e−12	4.8	2.0e−09
		−1,777 to −1,262	7.9	6.2e−13	5.0	8.3e−11
		−788 to −277	5.8	2.1e−07	3.7	2.1e−10
		−788 to −277	5.8	8.7e−13	3.5	1.2e−10
NM_004864	*GDF15*	−4,185 to −3,678	4.8	3.7e−11	3.5	7.7e−10
		−131 to +374	3.1	2.7e−08	ns	ns
NM_052815	*IER3*	−189 to +810	2.6	4.4e−08	ns	ns
NM_021127	*PMAIP1*	−781 to −260	3.9	7.0e−08	2.7	1.2e−07
		−45 to +1,021	2.6	4.4e−08	ns	ns
NM152877	*TNFRSF6*	−765 to −6	2.1	1.8e−06	ns	ns
		−765 to +421	4.6	4.1e−10	3.2	1.4e−08
		+14 to +984	6.4	8.3e−08	4.6	3.0e−10
		+862 to +1,371	3.2	2.3e−08	2.6	1.1e−06
NM_147187	*TNFRSF10B*	+220 to +739	10.9	6.3e−12	7.3	6.9e−12
Cell cycle/growth regulation						
NM_004060	*CCNG1*	−420 to +584	5.3	5.9e−12	3.9	3.9e−09
NM_078467	*CDKN1A*	−2,557 to −1,159	9.5	3.8e−13	7.8	1.3e−10
		−556 to −18	4.8	4.4e−10	3.5	2.1e−11
		+1 to +1,000	4.8	9.1e−11	2.9	1.3e−08
		+614 to +2,164	2.4	3.8e−10	ns	ns
NM_001274	*CHEK1*	−4,395 to −3,857	2.4	1.7e−07	ns	ns
NM_014398	*LAMP3*	−20 to +987	2.2	2.8e−09	ns	ns
NM_004073	*PLK3*	−945 to −184	9.1	1.9e−12	6.7	2.7e−12
NM_003620	*PPM1D*	−1,040 to −26	2.8	1.4e−08	2.2	2.6e−0.6
		+405 to +997	3.0	1.6e−0.7	2.3	9.1e−07
NM_152240	*WIG1*	−810 to −2	2.2	2.1e−09	ns	ns
		+192 to +694	2.8	1.6e−09	ns	ns
DNA damage response/repair						
NM_007306	*BRCA1*	−4,067 to −3,567	3.3	8.9e−09	2.7	4.7e−07
NM_001731	*BTG1*	−4,976 to −4,384	2.2	9.9e−08	ns	ns
NM_006763	*BTG2*	+1 to +1,000	3.6	4.2e−12	ns	ns
		+1 to +1,000	3.0	8.7e−07	ns	ns
NM_000107	*DDB2*	+51 to +955	8.6	1.6e−10	7.5	3.1e−11
NM_001924	*GADD45A*	+1 to +930	2.9	2.3e−08	ns	ns
		+1,026 to +2,060	6.1	6.7e−12	3.6	4.2e−09
NM_004628	*XPC*	−586 to −85	2.2	3.5e−07	ns	ns
Stress response						
NM_004024	*ATF3*	−304 to +817	2.1	4.0e−08	ns	ns
NM_024417	*FDXR*	+1 to +1,000	2.7	1.1e−10	ns	ns
NM_000581	*GPX1*	−522 to +1,384	3.5	1.8e−10	2.4	9.1e−08
NM_006253	*PRKAB1*	−112 to +942	4.8	2.0e−12	2.6	4.7e−08
NM_007233	*TP53AP1*	+93 to +867	2.2	8.0e−08	ns	ns
NM_147184	*TP53I3*	−543 to +212	2.7	5.3e−09	ns	ns
Other/unknown						
NM_001153	*ANXA4*	−797 to +654	2.2	1.3e−08	ns	ns
NM_020375	*C12orf5*	−245 to +755	4.7	3.6e−12	2.7	3.4e−07
NM_005191	*CD80*	−3,501 to −2,750	2.1	7.2e−09	ns	ns
NM_003512	*HIST1H2AC*	−4,966 to −4,332	2.8	4.7e−08	2.5	3.8e−06
NM_000528	*MAN2B1*	+1,014 to +2,151	2.0	9.5e−11	ns	ns
NM_000269	*NME1*	−306 to +239	4.3	5.0e−11	ns	ns
NM_012396	*PHLDA3*	−886 to −247	3.8	2.7e−10	2.6	2.0e−08
		−73 to +1,093	12.8	1.2e−11	8.1	2.0e−10
		+67 to +994	11.0	3.1e−12	7.0	2.8e−10
NM_004581	*RABGGTA*	−41 to +473	4.4	2.5e−10	2.5	1.2e−08
NM_002928	*RGS16*	−370 to +632	2.3	4.6e−08	ns	ns

(*Continued on the following page*)

Table 1. Genomic regions physically associated with p53 (Cont'd)

Accession no.	Gene	Probe position	4 h		24 h	
			Mean ratio	*P*	Mean ratio	*P*
NM_006513	*SARS*	+378 to +1,436	3.5	8.1e−10	2.4	5.6e−07
NM_003039	*SLC2A5*	−298 to +835	2.6	3.5e−10	ns	ns
NM_001252	*TNFSF7*	+29 to +956	2.1	6.9e−08	ns	ns

NOTE: Genes are grouped by functional classification. Probe positions are relative to the transcriptional start site of the corresponding gene. Mean ratio indicates the average signal from the immunoprecipitation-enriched DNA channel as compared with the average signal of the input control channel. *P* values are calculated from *t* tests for this comparison. ns, not significant by our testing criteria (Materials and Methods).

EDTA, 0.5 mmol/L EGTA, 0.25% Triton X-100, protease inhibitor cocktail]. Lysates were incubated for 15 minutes at room temperature with rotation and centrifuged; the pellet was resuspended in enrichment buffer [10 mmol/L Tris-Cl (pH 8.0), 200 mmol/L NaCl, 10 mmol/L EDTA, 0.5 mmol/L EGTA, protease inhibitor cocktail]. The preparation was incubated for an additional 15 minutes at room temperature with rotation. Insoluble material was pelleted, resuspended in 1 mL immunoprecipitation buffer [20 mmol/L Tris-Cl (pH 8.0), 200 mmol/L NaCl, 0.5% Triton X-100, 0.05% sodium deoxycholate, 0.5% NP40, protease inhibitor cocktail], and sonicated (Branson) to produce fragmented chromatin averaging ~500 bp in length. Fragmented chromatin was centrifuged to pellet the remaining insoluble material, and the supernatant was precleared overnight at 4°C with 1/20th volume magnetic protein-G beads (Dynal). The 1/20th volume was saved as input control. For each ChIP, either 1 μg anti-p53 antibody Ab-6 (Oncogene), 1 μg nonspecific immunoglobulin G (IgG; Sigma, St. Louis, MO), or no antibody was added and incubated for 8 hours at 4°C. Immune complexes were precipitated overnight at 4°C with 1/20th volume magnetic protein-G beads. Beads were washed three times with immunoprecipitation buffer, once with high salt buffer (immunoprecipitation buffer with 800 mmol/L NaCl), once in LiCl buffer [10 mmol/L Tris-Cl (pH 8.0), 250 mmol/L LiCl, 1% Triton X-100, 0.5% NP40, 0.1% sodium deoxycholate, 5 mmol/L EDTA, protease inhibitor cocktail], and twice with Tris-EDTA. Immune complexes were eluted with 50 μL elution buffer [10 mmol/L Tris-Cl (pH 8.0), 1% SDS, 5 mmol/L EDTA] at 65°C for 1 hour and cross-links were reversed by adding 200 mmol/L NaCl and incubating at 65°C overnight. Eluted material was treated with 30 μg proteinase K (Fisher, Pittsburgh, PA) for 2 hours at 42°C and purified (Qiagen, Valencia, CA).

Microarray fabrication. Primer pairs used to produce 1,267 human genomic DNA fragments were designed using Primer3. The genomic fragments were PCR amplified, ethanol precipitated, and resuspended in 3× SSC, 0.005% sarkosyl. PCR products were spotted onto aminosilane-coated glass slides (Cel Associates, Pearland, TX) using an Affymetrix 417 arrayer. Spotted DNA was covalently attached to the slide by UV cross-linking (Stratagene, La Jolla, CA) at 30 mJ followed by incubation at 80°C for 2 hours.

Probe preparation and microarray hybridization, washing, and scanning. Probe preparation and microarray hybridization were done essentially as previously described (11, 12). Briefly, immunoprecipitation-enriched genomic DNA and unenriched input DNA controls were subjected to ligation-mediated PCR to generate sufficient amounts of DNA for microarray hybridization. DNA preparation by ligation-mediated PCR and indirect DNA labeling with Cy3/Cy5 dyes via aminoallyl dUTP were done as previously described (12, 13). ChIP samples prepared from p53 ChIP or nonspecific IgG ChIP were labeled with Cy5 whereas input control DNA was labeled with Cy3. Hybridization of labeled DNA onto microarrays was as follows. Microarray slides were washed in 0.2% SDS, 2× SSC for 30 seconds, immersed in room-temperature water for 1 minute, and incubated in gently boiling water for 3 minutes. Slides were then dipped in ice-cold ethanol and spun dry. Labeled Cy3 and Cy5 DNA were combined and ethanol precipitated in the presence of 100 μg Cot-1 DNA. Precipitated DNA was dried and resuspended in 8 μL of 25 μg/μL yeast t-RNA and 30 μL of hybridization buffer (2× SSC, 0.1% SDS, 0.12% bovine serum albumin, 28% formamide, and 5.7% dextran sulfate). The hybridization mixture was incubated at 95°C for 5 minutes followed by 60°C for 30 minutes and hybridized onto the microarray at 60°C overnight. Microarrays were then washed in 0.1% SDS, 2× SSC for 10 minutes at 55°C, in 2× SSC for 10 minutes at room temperature, and in 0.2× SSC for 10 minutes at room temperature. Slides were spun dry and scanned on an Affymetrix 428 scanner.

Microarray data analysis. Background subtracted signal intensities from promoter microarrays were measured with ArrayVision 6.0 (Imaging Research, St. Catherines, Ontario, Canada). For each array, all intensities of the Cy5 (immunoprecipitation-enriched DNA) and Cy3 (unenriched input DNA) channels were scaled based on equalizing the intensities of the fluorophore channels for negative array elements. Negative array elements were defined as array elements displaying intensities in the 2nd quartile of lowest intensities in the Cy5 channel. Because the genomic regions that fail to show enrichment will yield low fluorescence signals on corresponding array elements in both fluorophore channels, this normalization scheme equalizes negative array elements without dampening enrichment signals in positive array elements. Genomic regions were considered to be occupied by p53 if both of the following criteria were satisfied: (*a*) the signal intensities of the corresponding array elements were significantly different between the p53 ChIP Cy5 channel and the input control Cy3 channel, with $P < 0.01$ for each comparison after correcting for multiple testing; and (*b*) the mean Cy5/Cy3 ratio was >2.

Quantitative PCR. Quantitation of DNA from p53 ChIP, nonspecific IgG ChIP, no antibody control, and input control was done with quantitative PCR reaction containing 12.5 μL SYBR green master mix (Qiagen), 7 μL water, 3 μL of 5 μmol/L primer mix, and 2.5 μL DNA. Quantitative PCR was carried out using an ABI 7000 Sequence Detection System, and primers were designed by Primer Express Software (Applied Biosystems, Foster City, CA). Comparisons were normalized to input controls.

Plasmids and luciferase reporter assay. Genomic fragments ~400 bp in size were cloned into pGL3-promoter vector (Promega, Madison, WI) and sequence verified. H1299 cells were grown to ~90% confluency in six-well plates and transfected with 2 μg of the appropriate vector and 0.5 μg of pRL-TK for 16 hours at 37°C. Transfections were done with Lipofectamine 2000 (Invitrogen, Carlsbad, CA) according to the suggestions of the manufacturer. Cells were kept at 37°C (mutant conformation) or shifted to 32°C (wild-type conformation) for an additional 24 hours. Cells were lysed and luciferase activity was assessed with Dual-Luciferase Reporter Assay System (Promega).

Results

Identification of genomic regions physically associated with p53 by location analysis. To identify ionizing radiation–responsive genes of which promoters are physically associated

Table 2. p53 binding motifs detected by p53MH

Gene	Sequence position	Site	Score	% Max	Sequence	Mean % input (4 h)
C12orf5	−1,245 to +1,755	**+411**	**25.86**	100.0	**AGACATGTCC AC AGACTTGTCT**	**1.09**
		−833	22.24	86.0	AGGCTTGTTA AAAA CGGCAAGACT	0.07
		+989	18.62	72.0	CGCCATGTTG GTC AGGCAGGTCT	0.29
GPX1	−1,522 to +2,384	+2,116	21.97	84.8	GGGCTTGTCT TTG AAGCCAGCTG	0.10
		−181	**21.23**	81.9	**GGGCCAGACC . AGACATGCCT**	**0.54**
		−700	20.06	77.4	AGGTTTGTTG AGTGCAAA GGACTAGCTT	0.34
PHLDA3	−1,073 to +2,093	−339	21.18	80.8	AAGCAAGCCC AC CCCCTTGCTA	0.53
		+691	**18.50**	70.5	**GGTCAAGTTC AAGAAC CAGCAGGCCA**	**1.48**
		+1,740	18.50	70.5	CGCCATGTTG GCC AGGCTGGTCT	0.23
PLK3	−1,945 to +816	−1,430	22.19	84.9	TACCTTGTTT AT CTGCTTGCCT	0.21
		−440	**20.60**	78.9	**TAACATGCCC GGGCAA AAGCGAGCGC**	**1.73**
		−961	18.48	70.8	AAATTAGCCG GGTGTGATG GCGCATGCCT	0.36
PRKAB1	−1,112 to +1,942	**+65**	**20.69**	80.0	**GTTCTTGCCG . CGGCTTGCCT**	**0.46**
		+57	19.50	75.4	CCCCTTGCGT TCTTGCCG CGGCTTGCCT	n.t.
		+75	18.51	71.6	CGGCTTGCCT . GGGCAGGTAA	n.t.
RABGGTA	−1,041 to +1,473	−22	20.49	79.0	CCGCAAGTCC CT CCCCAAGCCT	0.36
		+1,177	17.65	68.1	TGACAAGCCA GATTCTGGGAGCC AACCCTGATT	0.11
		+287	**16.13**	62.2	**CCTCTTGTGG AACGTGCA AAGCCTGTCC**	**1.23**
WIG1	−808 to +1,694	**+1,590**	**25.88**	100.0	**AAACAAGTCC . AGACATGCCT**	**3.99**
		+814	20.20	78.1	TACCTAGTTT GCTGAGGTGCTCC TAACCTGTTC	0.82
		−96	19.68	76.0	GGGCCTGCTC CGCCAA GCACATGCGC	0.34

NOTE: An algorithm, p53MH, was used to predict the p53 binding sites. "Sequence position" shows DNA sequences that were interrogated using p53MH; the positions are relative to the transcriptional start sites of the genes (National Center for Biotechnology Information built 33 of the human genome reference sequence). "Site" corresponds to the first base position of the predicted p53 binding site, "Score" and "% Max" are outputs from p53MH showing relative strength of the prediction. "Sequence" is that of the predicted site; a space is added in between sequence of spacer and those of the two decamer "half-sites" of p53 consensus element; a period represents no spacer in between decamers. ChIP was done using antibodies against p53 to validate the computational prediction. The sites showing largest enrichment experimentally are shown in bold. n.t., not tested due to overlapping sequences.

with p53, we did location analysis in a similar manner as previously reported (10–12). First, we irradiated human lymphoblastoid cells to induce p53 (Supplementary Fig. 1). Following ionizing radiation exposure, we collected the cells at 4 and 24 hours postirradiation and did ChIP assays with anti-p53 antibody. Immunoprecipitated genomic DNA regions associated with p53 were purified and labeled with Cy5 dye. Unenriched input DNA controls were collected and labeled with Cy3 dye. Parallel assays with nonspecific IgG antibody or no antibody were done as controls. Equal amounts of Cy5-labeled immunoprecipitation products and Cy3-labeled input DNA samples were cohybridized onto a microarray containing 1,267 DNA fragments representing the putative promoter regions of 489 ionizing radiation–responsive genes. The promoter regions of these genes are defined as 2 kb upstream to 1 kb downstream relative to the transcriptional start sites of the genes. Ten microarray replicates were done.

We considered genomic regions to contain p53 binding sites if the corresponding array elements displayed (*a*) significant differences ($P < 0.01$ by t test) in hybridization signals between the immunoprecipitation-enriched DNA channel as compared with the input control channel, and (*b*) the degree of enrichment was >2-fold. In total, at 4 hours postirradiation, 38 unique genes (~7.8%) represented by 55 array elements were significantly enriched ($P < 0.01$), and at 24 hours postirradiation, 19 genes (~3.9%) represented by 29 array elements were significantly enriched ($P < 0.01$) after Bonferroni correction for multiple testing (Table 1). The 19 genes that were enriched 24 hours postirradiation were a subset of the 38 genes enriched at the 4 hour time point. The degree of enrichment at 24 hours postirradiation was generally lower than that at 4 hours postirradiation. This observation may be explained by the decrease in p53 level at 24 hours as compared with p53 level at 4 hours (Supplementary Fig. 1). The specificity of our assay is high because we did not detect any array elements that displayed >2-fold intensity in the input channel over the p53 ChIP channel, nor did we observe enrichment for any genomic regions by ChIP with the nonspecific IgG antibody.

Among the 38 ionizing radiation–responsive genes that are associated with p53, many are involved in known p53 pathways such as DNA repair (*BRCA1*, *BTG2*, *DDB2*, and *XPC*), cell cycle regulation (*CDKN1A*, *CHEK1*, *GADD45A*, and *CCNG1*), and

apoptosis (*BAX*, *TNFRSF6*, and *TNFRSF10Ba*). However, a number of genes physically associated with p53 by location analysis are potential novel p53 targets.

Localization of p53 binding sites. Because the array elements range from 0.5 to 2 kb in size, the resolution of our location analysis was not able to pinpoint the precise position of p53 binding. Therefore, we carried out additional analysis to locate these sites for a set of ionizing radiation–responsive genes that was previously not known to be direct targets of p53.

First, we searched for possible p53 binding motifs within the p53-associated genomic regions using the p53MH algorithm (14). This program detects p53 binding motifs by scanning for the p53 consensus DNA binding sequence 5′-RRRCWWGYYY (N = 0-13) RRRCWWGYYY-3′, where R = purine, W = A or T, Y = pyrimidine, and N = any base. The sequences of each p53-associated genomic region, as represented on the microarray plus 1 kb of additional sequence flanking both the 5′ and 3′ ends, were analyzed. We tested the newly identified p53 target genes *C12orf5*, *GPX1*, *PHLDA3*, *PLK3*, *PRKAB1*, *RABGGTA*, and *WIG1*. p53MH provided several possible binding sites for each gene with scores indicating the likelihood of p53 binding (Table 2).

Next, we localized p53 binding for each gene by conventional p53 ChIP assays using irradiated cells and measured the extent of p53 association at the computationally predicted sites. For each gene, the region that was most enriched in the ChIP assay was identified as the p53 binding site (Table 2). The enrichment for the seven genes that were examined ranged from 0.5% to 4.0% of input DNA compared with 6.2 % of input DNA for *CDKN1A*, a known p53 target.

Ionizing radiation induces p53 binding. If p53 is indeed the transcriptional regulator of these ionizing radiation–responsive genes, we would expect to detect increased p53 binding to the promoter regions of these genes in response to ionizing radiation stress. As a result, we should also observe correlation between the extent of p53 binding and their gene expression levels.

To explore these scenarios, we used conventional ChIP assays to compare p53 occupancy at the promoters of *C12orf5*, *GPX1*, *PHLDA3*, *PLK3*, *PRKAB1*, *RABGGTA*, and *WIG1* for cells pre- and post-irradiation (Fig. 1). The previously identified promoters of *CDKN1A*, *DDB2*, and *GADD45A* were analyzed as positive controls whereas negative controls included exon 3 of *GAPDH* and a fragment 50 kb away from the previously characterized p53 binding site of *CDKN1A*. For all genes examined, with the exception of *WIG1*, p53 promoter occupancy significantly increased ($P < 0.05$) following ionizing radiation exposure as indicated by greater enrichment of p53-associated genomic DNA (Fig. 1). p53 promoter occupancy peaked at 4 hours postirradiation and declined by 24 hours postirradiation. For most genes, p53 promoter occupancy

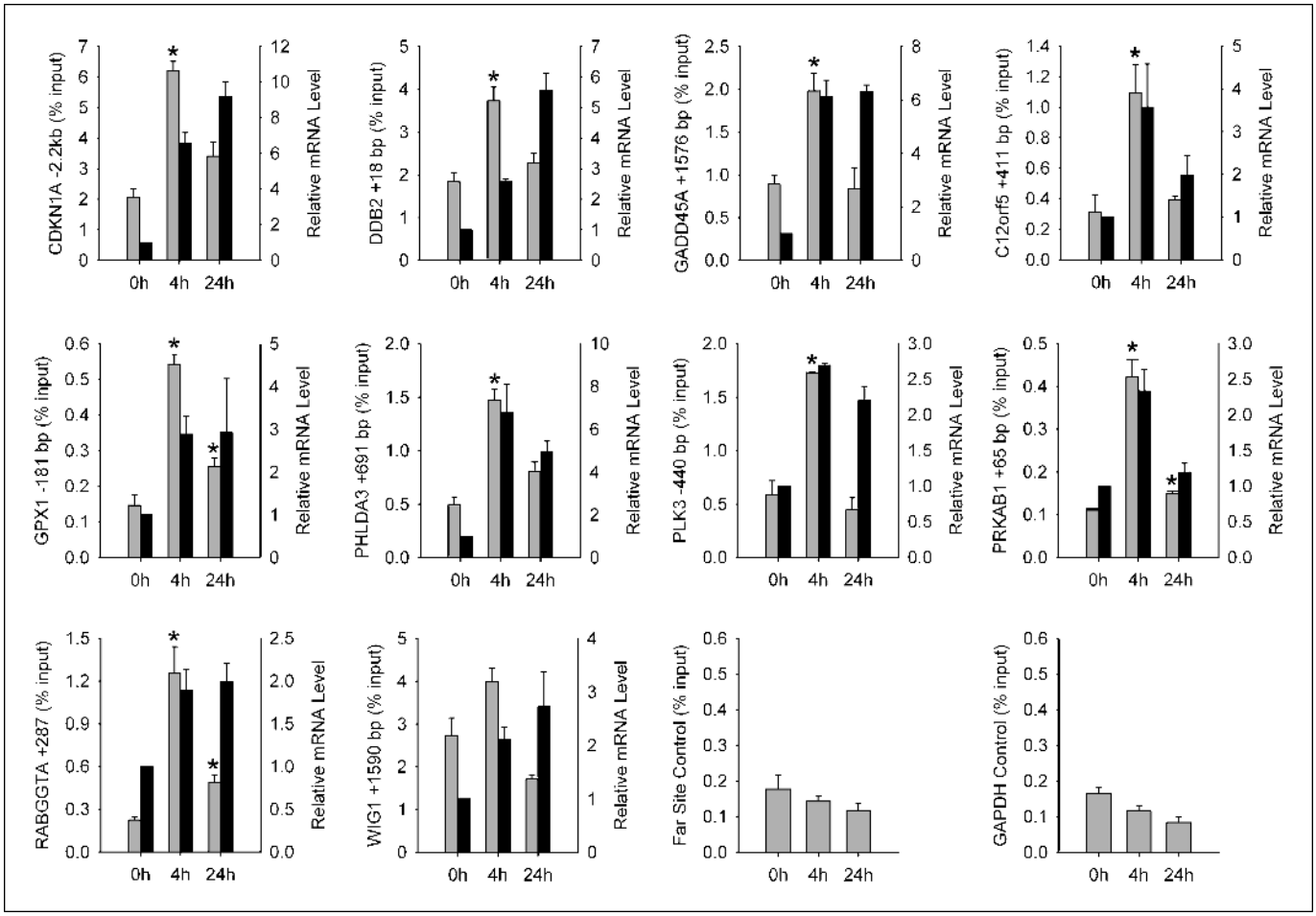

Figure 1. p53 binding to promoters of target genes as assessed by quantitative ChIP analysis. Amount of DNA recovered by p53 ChIP for cells before (0 hour) and following (4 and 24 hours) exposure to 10 Gy ionizing radiation (*gray columns*). *Asterisk,* significant difference as compared with 0 hour time point by *t* test ($P < 0.05$). Corresponding mRNA levels are indicated (*black columns*). *Bars,* SE for triplicate experiments.

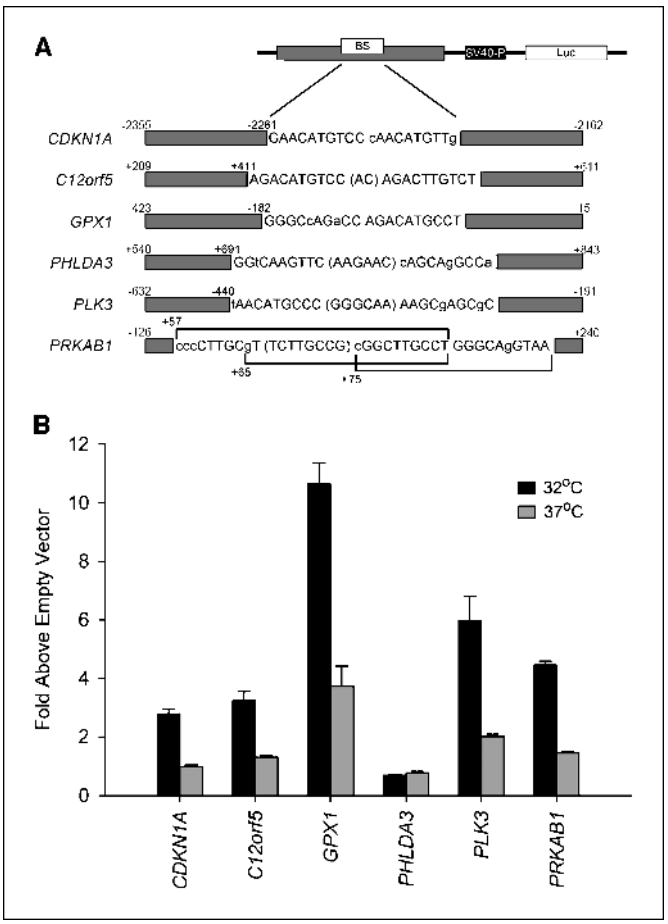

Figure 2. *C12orf5*, *GPX1*, *PLK3*, and *PRKAB1* possess p53-responsive elements. *A,* schematic of genomic segments cloned into pGL3-promoter luciferase reporter construct. Positions relative to the transcriptional start site for the genomic segments and the location of the p53 binding sites are indicated. Sequence of each p53 binding site is shown with mismatches to the p53 consensus binding sequence in lower case. Spacer nucleotides are bracketed. *B, C12orf5*, *GPX1*, *PLK3*, and *PRKAB1* reporter constructs are trans-activated by p53-Val138 in the wild-type conformation (32°C) but not in the mutant conformation (37 °C). *PHLDA3* reporter construct did not show p53-dependent *trans*-activation. *CDKN1A* promoter was used as a positive control. *Bars,* SE for triplicate experiments.

returned to basal levels by the 24 hour time point. No enrichment was observed for the negative controls.

We also assessed whether mRNA levels of these p53 target genes correlate with p53 occupancy following ionizing radiation exposure. We compared transcript levels at 4 and 24 hours after ionizing radiation exposure with those at the basal state (Fig. 1). At 4 hours postirradiation, we observed increases in mRNA levels that matched increases in p53 promoter occupancy. However, transcript levels remained elevated through the 24 hour time point whereas p53 binding declined. This difference in kinetics may result from a slower rate of mRNA decay as compared with the rate of synthesis. Taken together, these results indicate that p53 binds to the promoter regions of its target genes in an ionizing radiation–responsive manner and contribute to changes in their transcript levels following ionizing radiation exposure.

Functional p53-responsive elements. Because physical association of p53 with a genomic sequence in proximity to a gene does not necessarily imply direct transcriptional control of that gene by p53, we employed luciferase reporter assays to assess the functional legitimacy of these regions as p53-responsive elements. We tested the five newly identified p53 target genes, *C12orf5*, *GPX1*, *PHLDA3*, *PLK3*, and *PRKAB1*, by subcloning ~400 bp of genomic sequence containing the putative p53-responsive element into firefly luciferase reporter constructs (Fig. 2*A*). We also examined the previously characterized site for *CDKN1A* as a positive control. Each construct was transiently transfected into human H1299 cells that constitutively express temperature-sensitive mutant p53-Val138. At 37°C, p53-Val138 is maintained in the inactive mutant conformation and is unable to bind to p53-responsive elements. However, when the temperature is shifted to 32°C, p53-Val138 adopts a wild-type conformation and recovers p53 function (15).

The previously characterized p53-responsive element located 2.2 kb upstream from the *CDKN1A* transcriptional start site displayed *trans*-activation by p53-Val138 when shifted to 32°C whereas no *trans*-activation was observed for corresponding experiments at 37°C. Similarly, the luciferase reporter constructs for *C12orf5*, *GPX1*, *PLK3*, and *PRKAB1* exhibited *trans*-activation by functional p53-Val138 with minimal *trans*-activation by p53-Val138 in the mutant conformation (Fig. 2*B*). No *trans*-activation was observed for the *PHLDA3* reporter construct by functional or mutant forms of p53. These results show that p53-responsive elements are present in the corresponding genomic regions for the newly identified p53 target genes *C12orf5*, *GPX1*, *PLK3*, and *PRKAB1*.

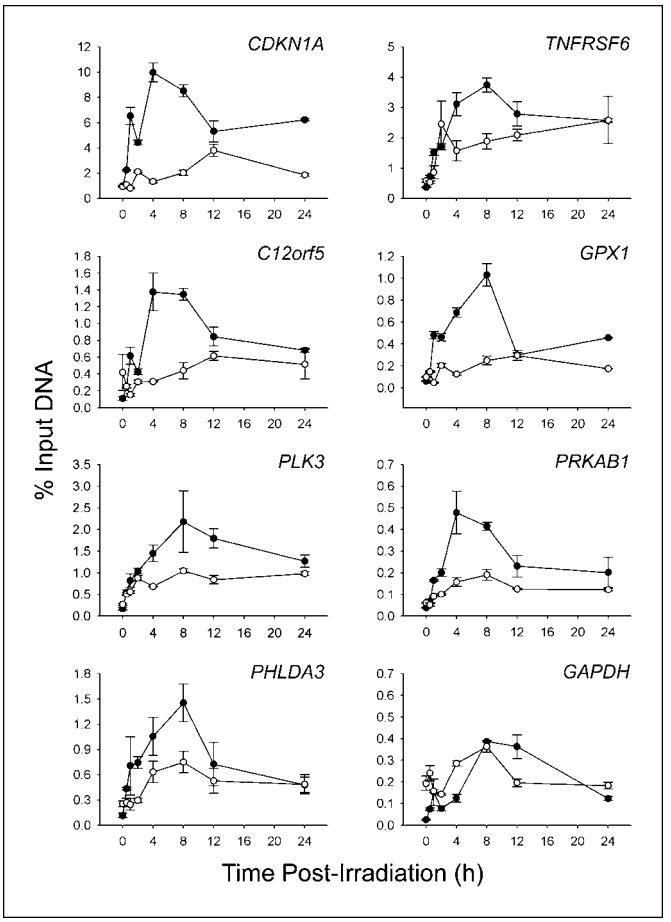

Figure 3. p53 occupancy at the promoter regions of target genes following ionizing radiation exposure. ●, $ATM^{+/+}$ cells; ○, $ATM^{-/-}$ cells. *Bars,* SE for triplicate experiments.

The p53-responsive elements are located in different areas relative to the transcriptional start site of each gene. The p53-responsive elements for *GPX1* and *PLK3* are within the first 500 bp region 5′ to their respective transcriptional start sites. In contrast, the p53-responsive element of *C12orf5* is within the first intron, and for *PRKAB1*, within the 5′ untranslated region. This observation is consistent with previously characterized p53-responsive elements and suggests that p53 biding sites often reside downstream to the transcriptional start site.

Ataxia telangiectasia cells display delayed and diminished p53 binding sites. We further examined p53 binding to the promoters of ionizing radiation–responsive genes by comparing p53 promoter occupancy in lymphoblastoid cells derived from normal individuals and in cells from patients with ataxia telangiectasia. We chose to use ataxia telangiectasia cells because these cells lack functional ATM, which acts as a key activator of p53. When triggered by ionizing radiation stress, ATM phosphorylates p53 and causes its dissociation from murine double minute 2. As a result, p53 is able to bind to the promoters of its target genes. However, ATM-dependent activation of p53 is defective in cells from ataxia telangiectasia patients.

We did quantitative ChIP assays to assess the kinetics of p53 occupancy at the promoters of *CDKN1A*, *TNFRSF6*, *C12orf5*, *GPX1*, *PLK3*, *PRKAB1*, and *PHLDA3* following exposure to 5 Gy ionizing radiation for both $ATM^{+/+}$ and $ATM^{-/-}$ lymphoblastoid cells. In all cases, $ATM^{+/+}$ cells displayed rapid increases in promoter occupancy by p53 as indicated by the amount of DNA enrichment corresponding to these genomic locations (Fig. 3). Binding of p53 to these regions peaked between 4 and 8 hours following ionizing radiation exposure and gradually declined through the 24 hour time point. In contrast, p53 binding to target genes, including *PHLDA3*, is delayed in $ATM^{-/-}$ cells (Fig. 3). The maximum level of p53 binding to target genes was lower in $ATM^{-/-}$ cells than in $ATM^{+/+}$ cells. *GAPDH* was used as a negative control and showed no appreciable changes in DNA enrichment or any differences between *ATM* genotypes (Fig. 3). These results suggest that p53 occupancy at the promoters of its target genes is delayed and diminished in $ATM^{-/-}$ cells. Consequently, transcriptional targets of p53 are not appreciably induced in $ATM^{-/-}$ cells following ionizing radiation exposure.

Discussion

In this study, we investigated promoter occupancy of 489 ionizing radiation–responsive genes by p53 and identified 38 direct transcriptional targets of p53. We observed ionizing radiation–dependent p53 binding and subsequent transcriptional activation of these genes using both *in vitro* and *in vivo* assays. Among these genes, some are previously reported as p53-regulated genes whereas the others are newly identified p53 targets. Our results add to the diverse roles that p53 plays in ionizing radiation–induced DNA damage response.

Among the newly identified p53 target genes, *PLK3* has been implicated in p53-associated pathways. *PLK3* encodes a serine/threonine kinase capable of phosphorylating a variety of targets, including p53 (16), CHEK2 (17), and CDC25C (18), following DNA damage. Unlike other polo-like kinases which promote cell cycle progression, PLK3 is a negative regulator of CDC25C. PLK3 is also involved in microtubule dynamics and centrosome function (19). Our data indicate that p53 can bind to the *PLK3* promoter and induce its expression following ionizing radiation exposure. Because p53 phosphorylation by PLK3 promotes p53 activity, induction of *PLK3* expression by p53 suggests a reciprocal regulatory scheme resulting in a positive feedback system to strengthen p53-related stress response in cell cycle regulation. Our results imply that p53 participates in G_2-M checkpoint activation through the inhibition of CDC25C via *PLK3* induction.

Another gene that we investigated is *GPX1*, which encodes an anti-oxidant protein. Following radiation exposure, cells accumulate highly reactive free radicals. Through induction of *GPX1*, p53 may be partially protecting cells from oxidative damage.

The putative promoter of *PHLDA3* exhibited enrichment by p53 ChIP. However, it did not show p53-dependent *trans*-activation in luciferase reporter assay. We further investigated p53 association with this gene by using irradiated lymyphoblastoid cells from normal individuals and ataxia telangiectasia patients. The binding of p53 to the *PHLDA3* promoter was greater in normal cells than in ataxia telangiectasia cells, which suggests that *PHLDA3* is a target gene of p53. The lack of *trans*-activation in transfection assay may be due to failure of the luciferase reporter system to recapitulate cellular environment. Similar observations have been reported by others; using the temperature-sensitive mutant p53-Val138 in the wild-type conformation, some promoters of p53 target genes such as *BAX* failed to be trans-activated (20). This confirms the need to use complementary techniques in various cell types to investigate transcriptional regulation.

In this study, we restricted our survey to genes with the previously characterized p53 consensus sequence and cells at two time points following exposure to 10 Gy ionizing radiation. Nevertheless, p53 binding is not always restricted to this consensus sequence. For example, p53 induces *TP53I3* by binding to a polymorphic pentanucleotide repeat within the 5′ untranslated region (21). At different ionizing radiation doses and time points, other genes are likely involved in the p53-dependent response. However, a preliminary survey of several p53 target genes in cells exposed to lower doses of ionizing radiation shows that they are also induced, but at a lower level (Supplementary Fig. 2). By extending our approach, which combines ChIP and reporter assays with computational tools, to time-course and dose-response experiments, one can begin to develop a comprehensive functional map of p53 and other transcription factors involved in radiation response.

Acknowledgments

Received 3/29/2005; revised 6/2/2005; accepted 6/23/2005.

Grant support: NIH grants HG02386 and GM070540, the W.W. Smith Endowed Chair (V.G. Cheung), and NIH training grant GM08216 (K-Y. Jen).

The costs of publication of this article were defrayed in part by the payment of page charges. This article must therefore be hereby marked *advertisement* in accordance with 18 U.S.C. Section 1734 solely to indicate this fact.

We thank Drs. Gerd A. Blobel, Greg H. Enders, Warren J. Ewens, Alan M. Gewirtz, and Haig H. Kazazian, Jr. for their comments and suggestions. We also thank Dr. Donna L. George for providing cell lines.

References

1. El-Deiry WS, Tokino T, Velculescu VE, et al. WAF1, a potential mediator of p53 tumor suppression. Cell 1993;75:817–25.
2. Tan T, Chu G. p53 Binds and activates the xeroderma pigmentosum DDB2 gene in humans but not mice. Mol Cell Biol 2002;22:3247–54.
3. Hollander MC, Alamo I, Jackman J, Wang MG, McBride OW, Fornace AJ Jr. Analysis of the mammalian gadd45 gene and its response to DNA damage. J Biol Chem 1993;268:24385–93.
4. Muller M, Wilder S, Bannasch D, et al. p53 activates the CD95 (APO-1/Fas) gene in response to DNA damage by anticancer drugs. J Exp Med 1998;188:2033–45.

5. Takimoto R, El-Deiry WS. Wild-type p53 transactivates the KILLER/DR5 gene through an intronic sequence-specific DNA-binding site. Oncogene 2000;19:1735–43.
6. Harris CC, Hollstein M. Clinical implications of the p53 tumor-suppressor gene. N Engl J Med 1993;329:1318–27.
7. Tusher VG, Tibshirani R, Chu G. Significance analysis of microarrays applied to the ionizing radiation response. Proc Natl Acad Sci U S A 2001;98:5116–21.
8. Amundson SA, Bittner M, Chen Y, Trent J, Meltzer P, Fornace AJ Jr. Fluorescent cDNA microarray hybridization reveals complexity and heterogeneity of cellular genotoxic stress responses. Oncogene 1999;18:3666–72.
9. Jen KY, Cheung VG. Transcriptional response of lymphoblastoid cells to ionizing radiation. Genome Res 2003;13:2092–100.
10. Ren B, Robert F, Wyrick JJ, et al. Genome-wide location and function of DNA binding proteins. Science 2000;290:2306–9.
11. Ren B, Cam H, Takahashi Y, et al. E2F integrates cell cycle progression with DNA repair, replication, and G(2)/M checkpoints. Genes Dev 2002;16:245–56.
12. Oberley MJ, Tsao J, Yau P, Farnham PJ. High-throughput screening of chromatin immunoprecipitates using CpG-island microarrays. Methods Enzymol 2004;376:315–34.
13. Ren B, Cam H, Takahashi Y, et al. E2F integrates cell cycle progression with DNA repair, replication, and G(2)/M checkpoints. Genes Dev 2002;16:245–56.
14. Hoh J, Jin S, Parrado T, Edington J, Levine AJ, Ott J. The p53MH algorithm and its application in detecting p53-responsive genes. Vol. 99, p. 8467–72, 2002.
15. Hirano Y, Yamato K, Tsuchida N. A temperature sensitive mutant of the human p53, Val138, arrests rat cell growth without induced expression of cip1/waf1/sdi1 after temperature shift-down. Oncogene 1995;10:1879–85.
16. Xie S, Wu H, Wang Q, et al. Plk3 functionally links DNA damage to cell cycle arrest and apoptosis at least in part via the p53 pathway. J Biol Chem 2001;276:43305–12.
17. Bahassi el, M, Conn CW, Myer DL, et al. Mammalian Polo-like kinase 3 (Plk3) is a multifunctional protein involved in stress response pathways. Oncogene 2002;21:6633–40.
18. Ouyang B, Li W, Pan H, Meadows J, Hoffmann I, Dai W, The physical association and phosphorylation of Cdc25C protein phosphatase by Prk. Oncogene 1999;18:6029–36.
19. Wang Q, Xie S, Chen J, et al. Cell cycle arrest and apoptosis induced by human Polo-like kinase 3 is mediated through perturbation of microtubule integrity. Mol Cell Biol 2002;22:3450–9.
20. Wang FJ. Analysis of downstream effectors of p53 on cell growth arrest and apoptosis induced by a temperature-sensitive Val138 mutant. J Med Dent Sci 1998;45:141–9.
21. Contente A, Dittmer A, Koch MC, Roth J, Dobbelstein M. A polymorphic microsatellite that mediates induction of PIG3 by p53. Nat Genet 2002;30:315–20.